v7.n9.2026

SCIENTIFIC JOURNAL - RECIMA21 ISSN 2675-6218

APPLICATION OF MOIRÉ OPTICAL TECHNIQUE AS HYBRID METHOD TO DETERMINEM STRESS AND STRAIN ON STRUCTURAL ELEMENTS UNDER FLEXURAL LOADING

ANÁLISE DO USO DA TÉCNICA ÓPTICA DE MOIRÉ COMO MÉTODO HÍBRIDO PARA DETERMINAÇÃO DO ESTADO DE TENSÃO E DEFORMAÇÃO EM ELEMENTOS ESTRUTURAIS SOB FLEXÃO

APLICACIÓN DE LA TÉCNICA ÓPTICA DE MOIRÉ COMO MÉTODO HÍBRIDO PARA DETERMINAR TENSIONES Y DEFORMACIONES EN ELEMENTOS ESTRUCTURALES SOMETIDOS A FLEXIÓN

Jonathan Gazzola[1], Kelen Cristiane Cardoso[2], Carlos Caetano de Almeida[3], Silvestre Rodrigues[4], Adilson Machado Enes[5], Ângelo Roberto Biasi[6], Inacio Mario Dal Fabbro[7]

e798960
https://doi.org/10.47820/recima21.v7i9.8960

PUBLISHED: 09/2026

ABSTRACT

The determination of stress and strain in agricultural sciences is of great importance. Biological materials are one of the areas involving machine design; however, they are complex from a material and geometric standpoint, making it difficult to use traditional methods of mechanical analysis to determine their stress-strain state. Optical techniques, such as moiré techniques, are known for determining full-field strain without distinction of geometric and material characteristics. The use of a hybrid methodology, through appropriate modeling, makes it possible to quantify the specific stress and strain state based on experimental body strain data. Therefore, this research work aims to analyze the use of phase-shifting moiré optical techniques as a method for determining the state of specific stress and strain in bodies under bending stress. The quantification of specific stress and strain was obtained through hybrid methodologies. The test specimen used was made of steel, fixed at both ends with an applied force at its mid-span with deflections ranging from 0.5 mm up to a limit of 2.5 mm. The results were compared with computer simulation data and electrical strain gauge technology. The results for specific strain were more satisfactory for intermediate applied load stages. For stress, the greater the deformations applied to the body, the closer the results were to computer simulation and electrical strain gauge. In general terms, the curve obtained by the moiré technique (MT) was closer to electrical strain gauges than to computer simulation. Finally, it was concluded that MT is feasible for use in determining forces, albeit with reservations for certain regions due to the complexity of the specific stress and strain curve produced by bending stress in loaded bodies, as well as edge errors and equipment constraints.

KEYWORDS: *Phase-Shifting Moiré. Photomechanic. Displacement Field. Stress-Strain Distribution. Hybrid Methods*.

[1] Agricultural Engineer from FEAGRI/UNICAMP. PhD in Agricultural Machinery from FEAGRI/UNICAMP. Associate Professor at CCA/UFSCar.
[2] Agricultural Engineer from UNICAMP. PhD in Agricultural Machinery from UNICAMP. Associate Professor at UNISO.
[3] Mechatronics Engineer from FEM/UNICAMP. PhD in Mechatronics Engineering from FEM/UNICAMP. Postdoctoral researcher in Digital Agriculture at DRNPA/UFSCar.
[4] Agricultural Engineer from UFLA. PhD in Agricultural Machinery from FEAGRI/UNICAMP. Full Professor at UFSJ.
[5] PhD in Agricultural Engineering from the University of Campinas, Brazil (2011). Permanent Professor at the Federal University of Sergipe.
[6] Degree in Logistics from UNIANHANGUERA. PhD in Agricultural Machinery from FEAGRI/UNICAMP. Postdoctoral researcher in Agricultural Engineering at FEAGRI/UNICAMP.
[7] Agronomist from ESALQ/USP. PhD in Agricultural Engineering from Michigan State University. Full Professor at FEAGRI/UNICAMP.

This article is published in open access under the Creative Commons Attribution 4.0 International (CC BY 4.0) license, which permits unrestricted use, distribution, and reproduction in any medium, provided that the original author and source are credited.

SCIENTIFIC JOURNAL - RECIMA21 ISSN 2675-6218

RESUMO
A determinação de tensão e deformação nas ciências agrárias é de grande importância. Os materiais biológicos constituem uma das áreas que envolvem projetos de máquinas, porém são complexos do ponto de vista material e geométrico, dificultando o uso de métodos tradicionais de análise mecânica para determinar seu estado de tensão-deformação. Técnicas ópticas, como as técnicas de moiré, são conhecidas por determinar a deformação de campo completo sem distinção das características geométricas e materiais. O uso de metodologia híbrida, por meio de modelagem adequada, se torna passível de quantificar o estado de tensão e deformação específica a partir dos dados experimentais de deformação do corpo. Logo, este trabalho de pesquisa visa analisar o uso de técnicas ópticas de moiré por phase-shifting como método para determinação do estado de tensão e deformação específica em corpos sob esforço fletor. A quantificação de tensão e deformação específica foi obtida por meio de metodologias híbridas. O corpo de prova utilizado foi feito de aço, biengastado em suas extremidades e com uma força aplicada em seu meio vão com deformações de 0,5 mm até o limite de 2,5 mm. Os resultados foram comparados com os dados de simulação computacional e a técnica de extensometria elétrica. Os resultados para deformação específica foram mais satisfatórios para estágios de meia carga aplicada. Para a tensão, quanto maiores as deformações aplicadas ao corpo, maior foi a proximidade dos resultados com a simulação computacional e a extensometria elétrica. Em termos gerais, a curva obtida pela TM foi mais próxima da extensometria elétrica do que da simulação computacional. Por fim, concluiu-se que a TM é passível de ser usada para determinação de esforços, porém, com ressalvas a algumas regiões devido à complexidade da curva de tensão e deformação específica que o esforço fletor produz nos corpos carregados, por erros de borda e restrição aos equipamentos utilizados.

PALAVRAS-CHAVE: Moiré por Phase-Shifting. Fotomecânica. Campo de Deslocamento. Estado de tensão e deformação. Metodologia Híbrida.

RESUMEN
La determinación de la tensión y la deformación en las ciencias agrarias es de gran importancia. Los materiales biológicos constituyen una de las áreas que involucran el diseño de máquinas; sin embargo, son complejos desde el punto de vista material y geométrico, lo que dificulta el uso de métodos tradicionales de análisis mecánico para determinar su estado de tensión-deformación. Las técnicas ópticas, como las técnicas de moiré, son conocidas por determinar la deformación de campo completo sin distinción de las características geométricas y materiales. El uso de una metodología híbrida, mediante un modelado adecuado, hace posible cuantificar el estado de tensión y deformación específica a partir de los datos experimentales de deformación del cuerpo. Por lo tanto, este trabajo de investigación tiene como objetivo analizar el uso de técnicas ópticas de moiré por desplazamiento de fase (phase-shifting) como método para la determinación del estado de tensión y deformación específica en cuerpos sometidos a esfuerzo de flexión. La cuantificación de la tensión y la deformación específica se obtuvo mediante metodologías híbridas. La probeta utilizada fue de acero, empotrada en sus dos extremos y con una fuerza aplicada en su luz (vano central) con deformaciones desde 0,5 mm hasta un límite de 2,5 mm. Los resultados se compararon con los datos de simulación computacional y la técnica de extensometría eléctrica. Los resultados de la deformación específica fueron más satisfactorios para las etapas de carga intermedia aplicada. En cuanto a la tensión, a mayores deformaciones aplicadas al cuerpo, mayor fue la proximidad de los resultados con la simulación computacional y la extensometría eléctrica. En términos generales, la curva obtenida por la técnica de moiré (TM) estuvo más cerca de la extensometría eléctrica que de la simulación computacional. Por último, se concluyó que la TM es apta para su uso en la determinación de esfuerzos, aunque con reservas en ciertas regiones debido a la complejidad de la curva de tensión y deformación

This article is published in open access under the Creative Commons Attribution 4.0 International (CC BY 4.0) license, which permits unrestricted use, distribution, and reproduction in any medium, provided that the original author and source are credited.

específica que el esfuerzo de flexión produce en los cuerpos cargados, así como por los errores de borde y las restricciones de los equipos utilizados.

PALABRAS-CLAVE: *Moiré por phase-shifting. Fotomecánica. Campo de desplazamiento. Estado de esfuerzo y deformación. Metodología híbrida.*

1. INTRODUCTION

The determination of the stress and strain state of a specimen subjected to mechanical loads is essential for machine design. Agricultural machinery constantly handles biological materials whose internal constitution classifies them as viscoelastic, and determining their stress state using traditional methods requires simplifying assumptions, leading to approximate data. Science must seek means to determine the stress and strain field with greater precision, and for biological materials, the use of optical techniques represents a viable alternative.

Traditional methods, such as computational tools, often struggle to simulate agricultural products due to their geometric and material complexity. Practical methods typically require the use of strain gauges, which can be costly, and their results may lack reliability due to experimental constraints.

Optical methods can measure surfaces without contacting the object and, when combined with photoelastic techniques, allow for the analysis of the specimen's stress and strain state. Combining optical techniques with classical photoelasticity concepts yields what are known as 'photomechanical techniques.' Among these, holography, dynamic speckle, and, more recently, the moiré technique stand out. The moiré technique is an optical method in which the intersection of fringes can generate the surface contour of an object, which can then be computationally vectorized. The difference between two surface contours of a loaded mechanical object—its deformed surface compared to its undeformed state—allows for obtaining the displacement field. Using equations based on object displacement makes it possible to determine its point-by-point stress-strain state. Thus, combining photomechanical techniques with classical mechanics equations is referred to as a 'hybrid methodology,' enabling the determination of an object's full stress-strain field.

In light of the above, the research question to be addressed is: Can the moiré technique be used to determine the stress and strain state of a body regardless of its material and geometric complexity? In this context, a reliable means to analyze the stress state of plant tissue bodies becomes necessary. The understanding of non-contact, high-precision optical surface analysis techniques, such as moiré, suggests that this methodology can bridge this gap. However, to

This article is published in open access under the Creative Commons Attribution 4.0 International (CC BY 4.0) license, which permits unrestricted use, distribution, and reproduction in any medium, provided that the original author and source are credited.

obtain a more definitive answer, this study applied the technique to a body with material and geometric linearity, comparing the findings with theoretical and practical results to determine their initial reliability. Therefore, this work serves as an initial case study with the potential for expansion based on the results obtained.

2. BIBLIOGRAPHIC REVIEW

In the agricultural sciences, the determination of stress and strain in biological materials is useful for predicting damage during the handling of plant tissues, developing and improving agricultural machinery and tools, as well as improving processes and controlling agricultural production. The analysis of critical stresses in horticultural products requires high-cost equipment and a specific experimental setup (ZULKIFLI *et al.*, 2020; SALARIKIA *et al.*, 2017; GAZZOLA *et al.*, 2021). The mechanical analysis of horticultural products, since they are viscoelastic materials, is time-dependent and affected by variations in moisture content, among other factors. Therefore, plant tissues are classified as rheological materials and are characterized by a heterogeneous internal structure and an irregular surface shape (MAHIUDDIN *et al.*, 2020; RASHVAND *et al.*, 2022). In this context, linear viscoelasticity is applied to obtain a more accurate representation of the stress and strain state, which makes its analysis more complex, particularly due to the material continuity issues involved. Therefore, the development of highly accurate methodologies for determining the stress and strain state in cellular structural elements is of considerable interest (STROPEK; GOLACKI, 2018). Mohsenin (1970) states that, due to the particularities of biological materials, the use of alternative methods for determining their stress and specific strain state is of great importance, such as optical methods, which include moiré techniques.

The use of computational tools is useful for analyzing the stress and strain state of an object. This technique is characterized as a full-field and theoretical analysis tool. However, its application to plant materials faces several challenges regarding modeling due to their geometric and material complexity (ZULKIFLI *et al.*, 2020; DAL FABBRO *et al.*, 2020). Rashvand *et al.* (2022) used computational simulation to analyze the mechanical behavior of fresh fruits and reported the need to introduce simplifications during the modeling process and to apply a finer mesh for the analysis, thus requiring a computer with greater processing capacity. Another widely used approach for mechanical analysis involves sensors for measuring deformation, such as accelerometers or strain gauges; however, this type of technique provides only local measurements (BAQERSAD *et al.*, 2017).

This article is published in open access under the Creative Commons Attribution 4.0 International (CC BY 4.0) license, which permits unrestricted use, distribution, and reproduction in any medium, provided that the original author and source are credited.

Optical techniques for analyzing mechanical behavior have been extensively investigated in recent decades due to advances in equipment, such as computers with more powerful software and processors, camera sensors, and related technologies. The use of optical techniques for mechanical analysis offers the advantages of being non-destructive and non-invasive, as well as being independent of geometric and material composition issues and providing full-field measurements (BAQERSAD *et al.*, 2017; DAL FABBRO *et al.*, 2020).

Among optical techniques, the phase-shifting moiré technique (MT) has attracted particular attention because it is simple, provides full-field measurement data, is non-contact, is less susceptible to noise, has a low cost, and offers good reliability (GOMES *et al.*, 2009; FUJITA; ARAKI, 2021). MT is based on the projection of four gratings onto the specimen, whose interference, obtained through image processing, results in the contour profile of the object. The difference in the out-of-plane surface contour between the deformed and undeformed specimens provides displacement data, which are proportional to strain, thereby establishing MT as a photomechanical technique (BRUNO, 2018; SRIKLIN *et al.*, 2017). The quantification of stress and strain is achieved using a hybrid methodology, which combines strain data measured by experimental techniques with mathematical models and equations (DOYLE, 2008). Sriklin *et al.* (2017) used continuum mechanics equations together with full-field deformation data obtained using the moiré technique to determine the stress and strain state of an object, obtaining satisfactory results.

Based on the considerations presented above, this research aimed to analyze the use of the phase-shifting moiré technique as an optical method for determining stress and strain in specimens subjected to loadings. Stress and strain were quantified using a hybrid methodology. The results obtained using MT were compared with data from computational simulations and electrical strain gauge measurements to assess the reliability of the technique. The results achieved may serve as an initial step for application in materials of greater complexity, such as biological materials.

3. MATERIAL AND METHODS

The hybrid methodology adopted for this experiment consisted of using the phase-shifting moiré optical technique to determine the displacement field, alongside classical mechanics equations to determine the stress and specific strain field. The experimental tests were carried out at the Laboratory of Optics, located at the Faculty of Agricultural Engineering of UNICAMP, Campinas, SP, Brazil. The test specimen consisted of a 1020 carbon steel piece with dimensions

This article is published in open access under the Creative Commons Attribution 4.0 International (CC BY 4.0) license, which permits unrestricted use, distribution, and reproduction in any medium, provided that the original author and source are credited.

of 165.00 mm in total length for clamping, 12.70 mm in width, and 1.00 mm in thickness, as required by the ASTM E855-08 standard. However, that standard specifies a gauge length of 100.00 mm. The experimental procedure was divided into four steps, namely: (1) mechanical loading test; (2) optical testing and image processing; (3) stress and strain determination; and (4) comparative testing.

3.1. Mechanical Loading Test

Mechanical loading was applied to a beam clamped at both ends. A custom testing device, shown in Figure 1, was developed to hold the specimen in a vertical position and apply a bending moment under displacement-controlled mechanical loading. In this study, five displacement levels were applied to the specimens: 0.5 mm, 1.0 mm, 1.5 mm, 2.0 mm and 2.5 mm. A Mitutoyo Model 543-682 digital dial indicator with a precision of 0.01 mm was placed at the mid-span of the beam to measure maximum deflection. The metallic specimens were painted opaque white to improve contrast with the projected grids. The tests were carried out with five replications. The base of the testing device was firmly clamped to a table to prevent unwanted movement during load application. The laboratory lights were turned off, and the windows and doors were covered with dark fabric to prevent ambient light penetration.

Figure 1. Testing device for bending moment application. Source: Author, 2026

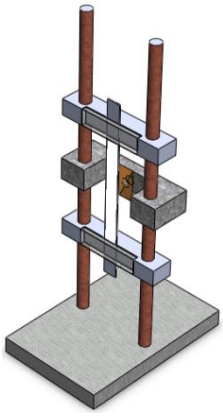

3.2. Optical testing and image processing

This research selected Phase-Shifting Moiré as the optical method to obtain the full-field deformation. The optical setup included a Samsung 6.4-megapixel digital camera with a remote control to capture images without unwanted movement, and an Epson multimedia projector

This article is published in open access under the Creative Commons Attribution 4.0 International (CC BY 4.0) license, which permits unrestricted use, distribution, and reproduction in any medium, provided that the original author and source are credited.

connected to a PC to project the optical grids onto the specimen surface. The optical grid had a period of 0.2 mm. Both the projector and the PC had their resolution set to 1024 × 768 to prevent unwanted noise. Figure 2 shows the setup required for the Phase-Shifting Moiré optical technique.

Figure 2. Experimental setup for phase-shifting moiré tests. Source: Author, 2026

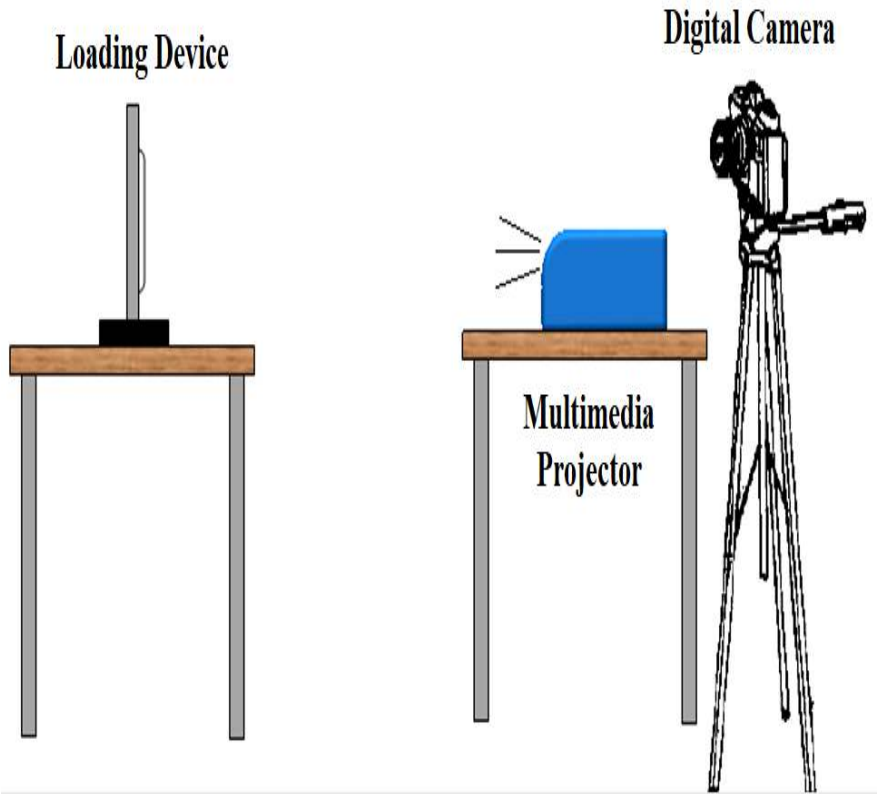

The image acquisition procedure was carried out as follows: First, Fringe Projection software was used to generate optical grids. Then, four optical grids with a period of 0.2 mm and phase shifts of 90°—designated as $g_1(x,y)$, $g_2(x,y)$, $g_3(x,y)$ and $g_4(x,y)$—were projected onto the reference (unloaded) beam surface, and the corresponding images were recorded. Sequentially, one of the grids was projected onto the deformed beam surface for each deformation level, and the image was captured and recorded. One image was required for each displacement step. Each image of the deformed body was named $I_n(x,y)$, where n represents the displacement level ranging from 0.5 mm to 2.5 mm (n = 0.5, 1.0, 1.5, 2.0 and 2.5 mm), resulting in a set of nine images for the complete test. The optical tests were performed with five replications. Next, the

This article is published in open access under the Creative Commons Attribution 4.0 International (CC BY 4.0) license, which permits unrestricted use, distribution, and reproduction in any medium, provided that the original author and source are credited.

image processing procedure was initiated to determine the specimen deformation field. This procedure was conducted according to Santos *et al.* (2020) using ImageJ and Scilab 4.1.1 software. Initially, the images from each loading test were opened in ImageJ for pre-processing, which included RGB-to-grayscale conversion, noise removal, definition of the region of interest (ROI), and application of filters to improve the contrast of the fringe patterns. A Gaussian Blur filter was applied during this stage. A routine was developed to automate this processing sequence while maintaining consistent reference points for fringe formation. Subsequently, using ImageJ, the pre-processed images were further analyzed to generate interference patterns and obtain Moiré fringes on the specimen surface at each loading stage. For this purpose, the Difference operation was performed using Equations 01 to 04, as shown below:

$$m_1(x,y) = g_1(x,y) - I_n(x,y) \quad (01)$$

$$m_2(x,y) = g_2(x,y) - I_n(x,y) \quad (02)$$

$$m_3(x,y) = g_3(x,y) - I_n(x,y) \quad (03)$$

$$m_4(x,y) = g_4(x,y) - I_n(x,y) \quad (04)$$

Where $I_n(x,y)$ represents the image corresponding to each imposed displacement (n) applied to the specimen and $m_n(x,y)$ represents the image resulting from the processing. Thus, for each specimen test, four images were generated for each imposed deformation, resulting in a total set of 20 images. The images were saved in BMP format.

The third stage of the image processing procedure comprised processing the images to generate the full-field displacement, using Scilab 4.1.1 software. The deformed surface topography was obtained using Equation (5).

$$R_n(x,y) = \arctan \{ [m_4(x,y) - m_2(x,y)] / [m_1(x,y) - m_3(x,y)] \} \quad (05)$$

The image generated at that step for each imposed deformation n was named $R_n(x,y)$, which was forwarded to the ImageJ software to initialize the last step, i.e., the topographic elevation throughout the beam length. In this step, image $R_n(x,y)$ was filtered by a Gaussian Blur filter to smooth the deformation curve. Then, a line crossing the image length was plotted and the Plot Profile command generated a deformation curve based on pixel intensity, as shown on Figure 3 and the displacement curve data were saved in XLS format.

This article is published in open access under the Creative Commons Attribution 4.0 International (CC BY 4.0) license, which permits unrestricted use, distribution, and reproduction in any medium, provided that the original author and source are credited.

Figure 3. Obtaining the specimen's strain curve: a) Plotting the analysis line; b) Strain curve in pixel intensity. Source: Author, 2026

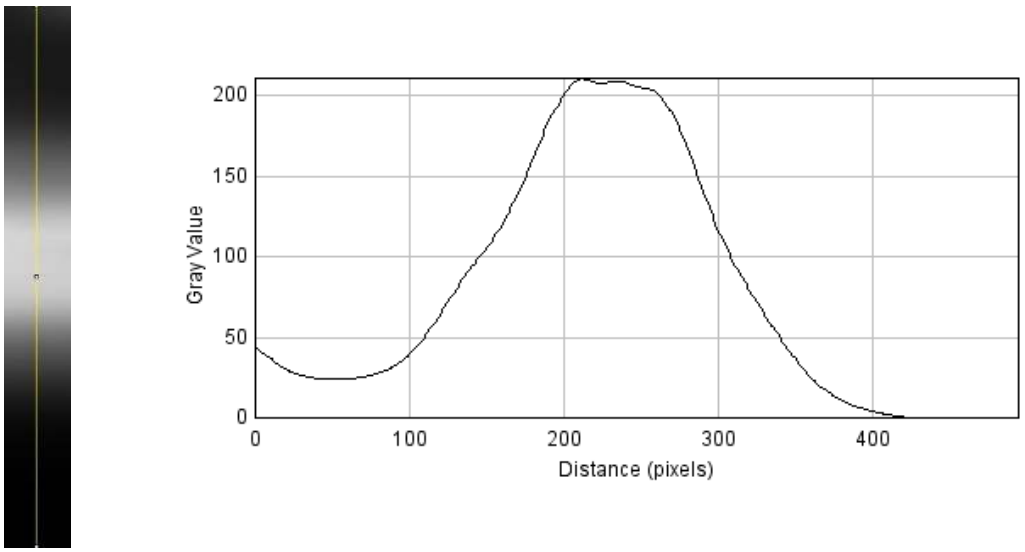

a) b)

3.3. Stress and strain determination

The next step involved converting data from pixels to millimeters using Microsoft Excel software. The pixel-to-millimeter ratio established at the displacement-controlled point — specifically at the beam mid-span — allowed for the numerical displacement values to be determined across the entire beam length. Once the deflection curve data (Z) were converted, the specific strain (ε_{11}) was calculated using Equation 06. Subsequently, using 1D Hooke's Law in conjunction with the manufacturer-supplied modulus of elasticity (E) for 1020 steel (200 GPa), the normal stress in the beam (σ_{11}) was calculated via Equation 07.

$$\varepsilon_{11} = 12.Z.h / L^2 \quad (06)$$

$$\sigma_{11} = E.\ \varepsilon_{11} \quad (07)$$

Where h is the metallic beam height and L is the testing length, both in millimeters.

This article is published in open access under the Creative Commons Attribution 4.0 International (CC BY 4.0) license, which permits unrestricted use, distribution, and reproduction in any medium, provided that the original author and source are credited.

3.4. Comparison Tests

To validate the results obtained by Phase-Shifting Moiré (PSM), two comparative evaluations were performed: (1) finite element simulation, and (2) strain gauge testing. The computational simulation provided the expected theoretical stress and strain fields based on continuum mechanics under the same boundary and loading conditions as the optical test. In turn, electrical strain gauging was selected as an experimental benchmark to measure the mechanical stresses in the beam, given its widespread use as a standard reference technique. The computational simulation aimed to replicate the experimental optical setup in a virtual environment. This included the specimen geometry (length = 100.0 mm; width = 12.7 mm; thickness = 1.0 mm), isotropic material properties (E = 200 GPa and v = 0.29), mid-span displacement application, and fixed boundary conditions at both ends. The displacements applied to the virtual beam matched the experimental levels (n = 0.5, 1.0, 1.5, 2.0 and 2.5 mm). The simulation was conducted in Abaqus 6.10 using a bottom-up mesh with 1,000 nodes, and non-linear numerical convergence was achieved via the Newton-Raphson method. A linear elastic constitutive model was adopted. The resulting stress and strain profiles along the specimen length were exported as datasets relating spatial position (X-axis) to the corresponding mechanical response (Y-axis), which were subsequently plotted using Microsoft Excel. The electrical strain gauge testing was performed using a universal testing machine. Five specimens were evaluated in this experimental stage. Five KYOWA KFG-5-120-C1-1 strain gauges were bonded to the back surface of each specimen — excluding the clamped ends, where mounting was not feasible — as shown in Figure 4.

Figure 4. Strain gauge positions on the metallic beam surface. Distance in mm. Source: Author, 2026

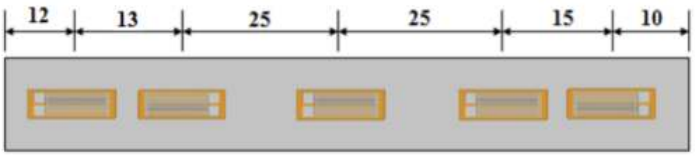

The specimen displacement at the load application point was monitored using a dial indicator. A data acquisition system comprising a SYSTEM 5000 receiver and StrainSmart MG 5000 software was used to record both the dial indicator displacement and the strain data. Equations 08, 09, 10 and 11 were used to calculate the moment of inertia (I), the estimated applied

This article is published in open access under the Creative Commons Attribution 4.0 International (CC BY 4.0) license, which permits unrestricted use, distribution, and reproduction in any medium, provided that the original author and source are credited.

force (P), bending moment (M), and longitudinal strain (ε_{11}), respectively. The stress state (σ_{11}) was subsequently determined from the experimental strain data using Equation 12.

$$I = b.h^3/12 \quad (08)$$

$$P = 192.E.I.\Delta / L^3 \quad (09)$$

$$M = P.L / 8 \quad (10)$$

$$\varepsilon_{11}=M.y/E.I \quad (11)$$

$$\sigma_{11} = \{[E.(1-v)] / [(1+v).(1-2v)]\} . \varepsilon_{11} \quad (12)$$

Where Δ is the local deflection of the beam, in millimeters, and y is the distance from the neutral axis.

4. RESULTS AND DISCUSSION

Figures 5 to 9 present the strain distributions obtained from the experimental and numerical evaluations. The graphs compare the results for each test condition using the Moiré Technique (MT), finite element simulation, and electrical strain gauging. The strain gauge curves were plotted only along the region where sensor attachment was feasible. Furthermore, these curves represent the average of the five test replications, as the experimental measurements exhibited minimal scatter. To enable a clearer comparison with the MT results, the mean values were calculated for each measurement point to construct the representative strain curves for the strain gauge testing.

Figure 5. Strain curve result under displacement of 0.5 mm. Source: Author, 2026

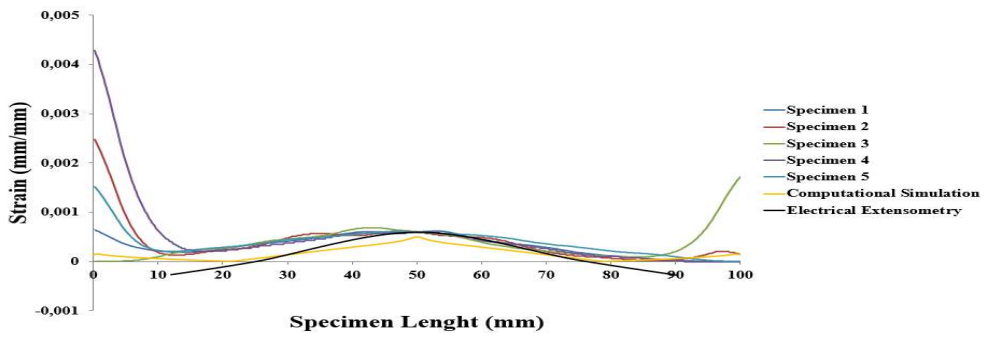

This article is published in open access under the Creative Commons Attribution 4.0 International (CC BY 4.0) license, which permits unrestricted use, distribution, and reproduction in any medium, provided that the original author and source are credited.

Figure 6. Strain curve result under displacement of 1.0 mm. Source: Author, 2026

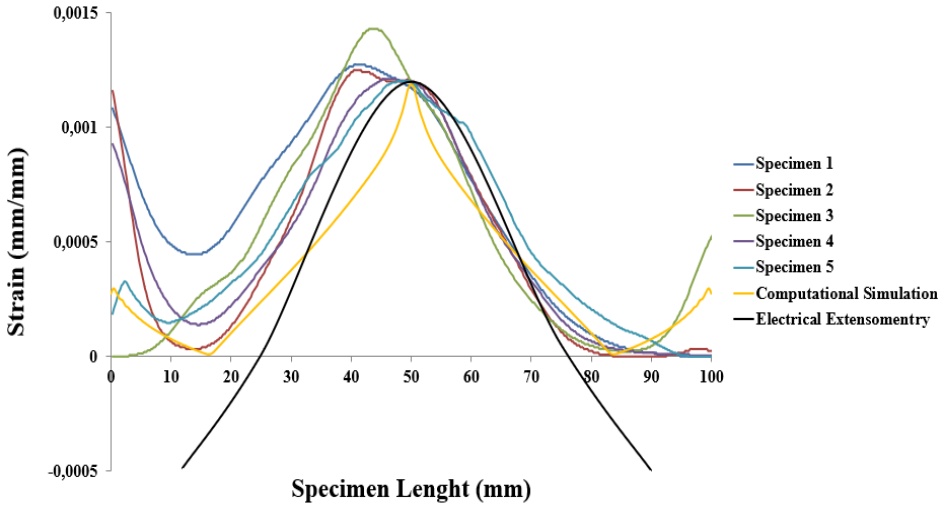

Figure 7. Strain curve result under displacement of 1.5 mm. Source: Author, 2026

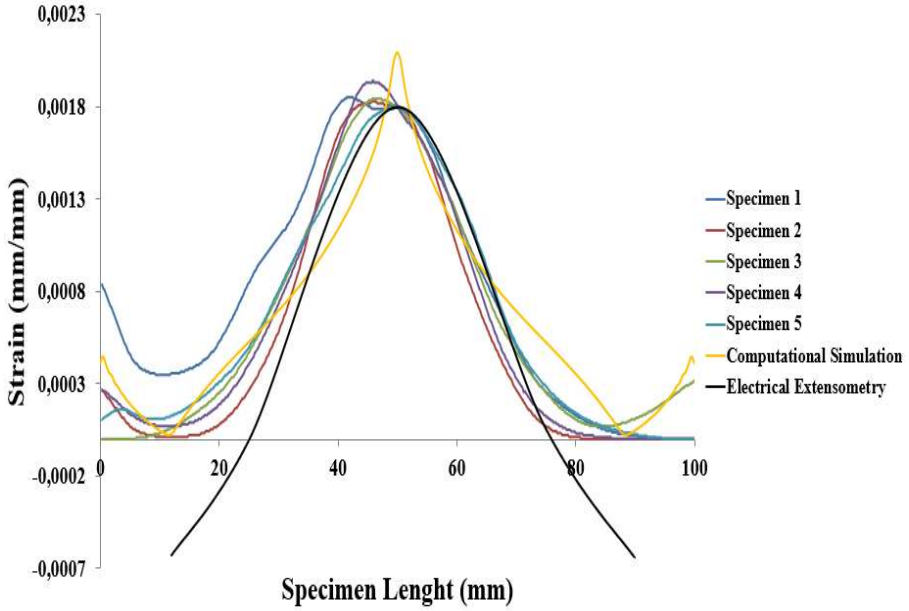

This article is published in open access under the Creative Commons Attribution 4.0 International (CC BY 4.0) license, which permits unrestricted use, distribution, and reproduction in any medium, provided that the original author and source are credited.

Figure 8. Strain curve result under displacement of 2.0 mm. Source: Author, 2026

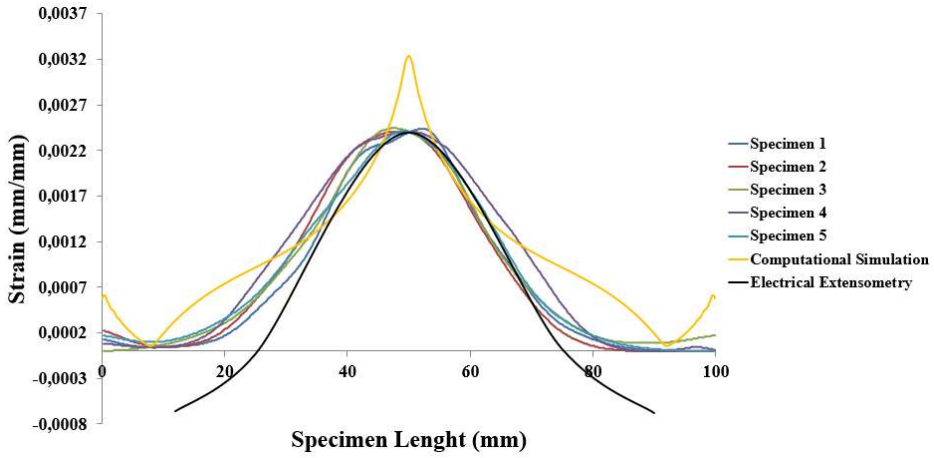

Figure 9. Strain curve result under displacement of 2.5 mm. Source: Author, 2026

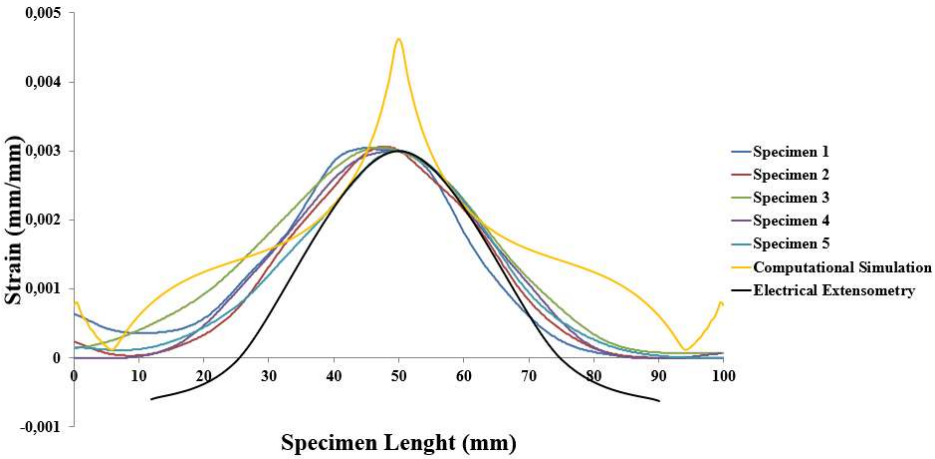

Figures 10 to 14 present the stress distributions (MPa) obtained from the evaluations. The graphs compare the results for each test condition using the Moiré technique, finite element simulation, and electrical strain gauging. The plotting procedure adopted for the stress profiles was identical to that used for the strain distributions.

This article is published in open access under the Creative Commons Attribution 4.0 International (CC BY 4.0) license, which permits unrestricted use, distribution, and reproduction in any medium, provided that the original author and source are credited.

Figure 10. Stress curve result under displacement of 0.5 mm. Source: Author, 2026

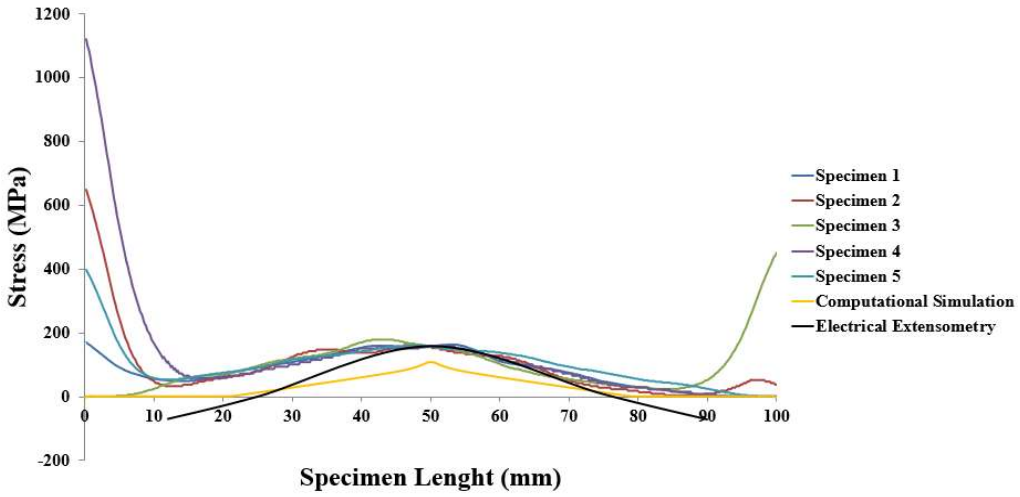

Figure 11. Stress curve result under displacement of 1.0 mm. Source: Author, 2026

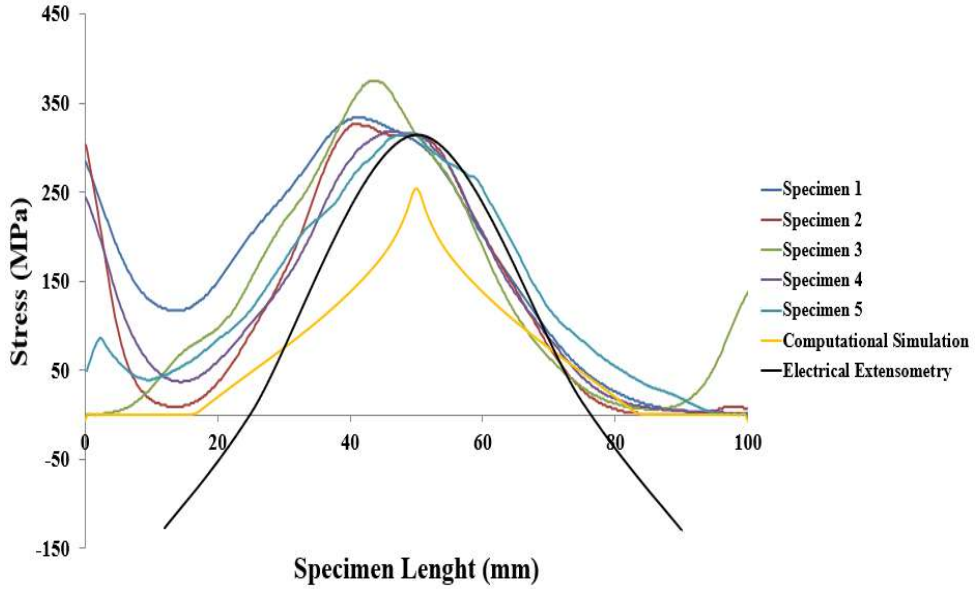

This article is published in open access under the Creative Commons Attribution 4.0 International (CC BY 4.0) license, which permits unrestricted use, distribution, and reproduction in any medium, provided that the original author and source are credited.

Figure 12. Stress curve result under displacement of 1.5 mm. Source: Author, 2026

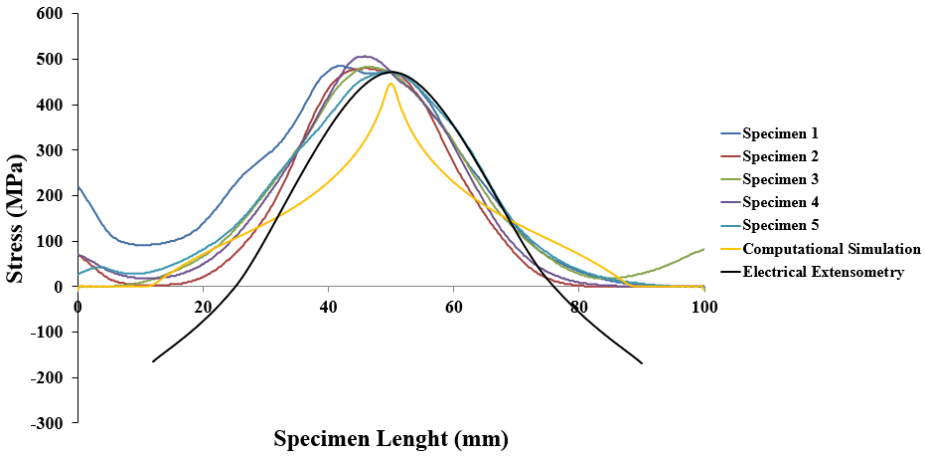

Figure 13. Stress curve result under displacement of 2.0 mm. Source: Author, 2026

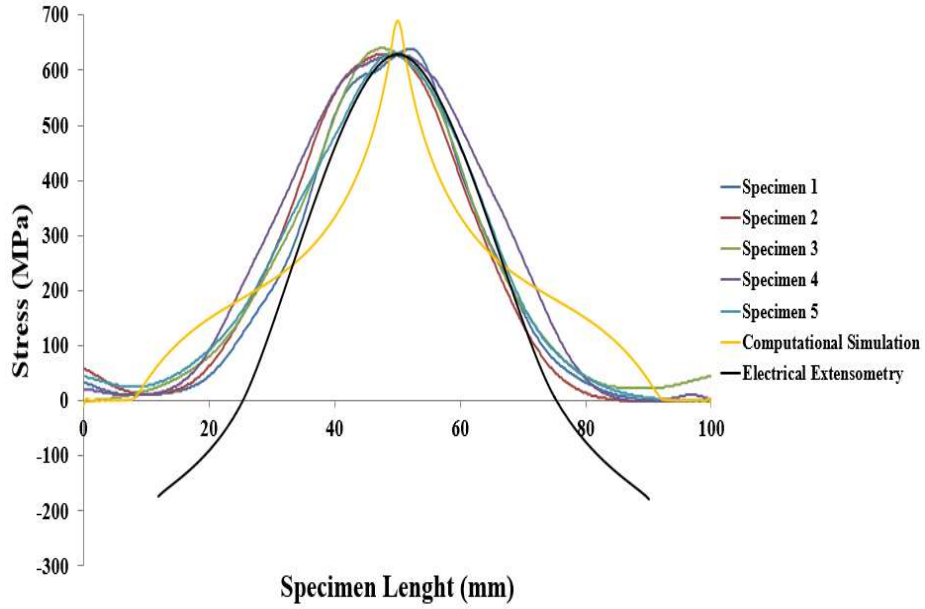

This article is published in open access under the Creative Commons Attribution 4.0 International (CC BY 4.0) license, which permits unrestricted use, distribution, and reproduction in any medium, provided that the original author and source are credited.

Figure 14. Stress curve result under displacement of 2.5 mm. Source: Author, 2026

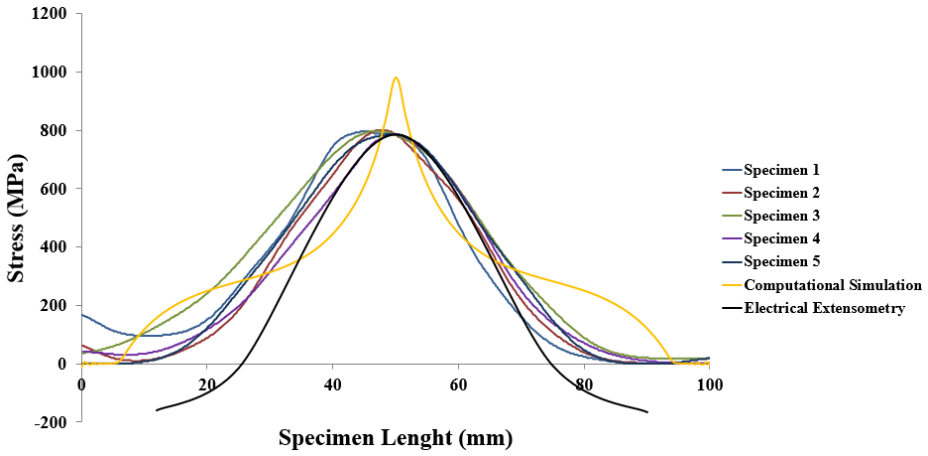

An overall analysis of the strain and stress results demonstrates that the Phase-Shifting Moiré (PSM) technique yielded data in reasonable agreement with the benchmark methods. In the mid-span region, the non-linear profile of the strain curve obtained by PSM closely matched that measured by electrical strain gauging. Conversely, near the clamped ends, the PSM results aligned more closely with the finite element simulation, which captured the zero-crossing inflection points prior to the magnitude increase at the supports. The stress profiles exhibited a similar response; notably, PSM yielded near-zero stress at the right support, whereas the computational model predicted symmetric near-zero values at both supports. The non-zero stress observed via PSM at the left support is attributed to edge artifacts, as discussed below. Regarding discrepancies between the experimental methods, a noticeable divergence in curve topology occurred near the specimen boundaries.

Electrical strain gauging measured negative strain and stress magnitudes, a phenomenon absent in both the PSM and numerical results. Although negative values were unexpected based on the idealized computational model, physical observations during testing confirmed that the specimen curvature matched the strain gauge readings.

Discrepancies between theoretical predictions and strain gauge measurements under similar clamped boundary conditions were also reported by Sanchez-Espiga *et al.* (2022) and are primarily associated with support compliance and clamping friction in the fixture. Furthermore, the PSM formulation cannot inherently represent negative deformation values due to the non-negative nature of digital pixel intensity fields. Stress and strain profiles predicted by the numerical simulation exhibited steeper gradients and higher spatial curvature than the experimental results,

This article is published in open access under the Creative Commons Attribution 4.0 International (CC BY 4.0) license, which permits unrestricted use, distribution, and reproduction in any medium, provided that the original author and source are credited.

featuring a sharp peak in the central loaded region. According to Timoshenko and Gere (1984), localized peak stresses are theoretically expected when material yielding or localized plastic deformation occurs. Similarly, Silva *et al.* (2012) observed notable deviations between experimental bending data and theoretical models, particularly in regions distant from the load application point.

A critical evaluation of the PSM technique indicates that the most reliable measurements were obtained in the central span of the specimen. At the specimen boundaries, measurement errors were driven by optical edge artifacts. These boundary distortions stem from non-uniform illumination gradients—as reported by Braga *et al.* (2009)—and spatial filtering artifacts, particularly from applying Gaussian blurring near image borders during pre-processing (SILVA *et al.*, 2017). Notably, these edge distortions became less dominant at higher displacement levels, corroborating the findings of Nigam and Singh (2020). The applicability of PSM is strongly governed by the magnitude of the applied displacement.

The reconstructed field became smoother and more continuous at higher deflection levels — specifically at n = 2.0 mm and 2.5 mm — where the fringe contrast was significantly enhanced. This behavior is inherent to optical interferometry: larger out-of-plane displacements increase the spatial phase shift between the reference and deformed grating patterns, yielding higher visibility and signal-to-noise ratio in the fringe fields. Another limiting parameter was the spatial period of the projected optical grid, which was restricted to a pitch of 0.2 mm due to resolution limits of the projector. A similar hardware constraint was documented by Hubble and Weaver (2017). Projecting higher-density grids induced parasitic Moiré patterns during the projection phase itself due to pixel aliasing and interpolation from the display engine. These anti-aliasing artifacts introduced non-uniform spatial noise across the specimen surface. Mitigating these interpolation artifacts required stronger Gaussian filtering, which inadvertently amplified boundary distortion effects. Future work should focus on utilizing higher-resolution optical projection systems to minimize hardware-induced spatial artifacts.

5. CONCLUSION

Based on what was presented above, this research allows concluding that for the phase-shifting moiré technique: 1 – The stress and strain curve was consistent with the curve obtained by electrical strain gauging, confirming the experimental nature of the MT. At the ends, the MT was in agreement with the computer simulation. This observation

This article is published in open access under the Creative Commons Attribution 4.0 International (CC BY 4.0) license, which permits unrestricted use, distribution, and reproduction in any medium, provided that the original author and source are credited.

leads to the conclusion that the stress and strain behavior obtained by the moiré technique are experimental in nature, which reinforces the importance of using this technique for non-destructive testing. Assuming that the experimental results showed a high correlation, it can be stated that the moiré technique, when combined with the hybrid methodology, was effective in determining the stress and strain curve; 2 – The MT shows greater effectiveness in analyses as specimen strain increases; 3 – Using equipment with higher resolution can improve the quality of the results obtained, serving as a topic to be explored in future work.

Despite the discrepancies that occurred and considering the agreements achieved, the phase-shifting moiré technique combined with the hybrid methodology demonstrated reliability in the results obtained, noting that the strain and stress data at the most heavily loaded points were close to the values obtained by the comparative techniques analyzed. Therefore, it is concluded that the phase-shifting moiré technique was viable for the qualitative determination of stress and strain.

ACKNOWLEDGEMENTS

This work was supported by UFSCar Center for Agricultural Sciences (CCA) – project FAI RTI-CCA.

REFERENCES

BAQERSAD, J. *et al.* Photogrammetry and optical methods in structural dynamics – A review. **Mechanical Systems and Signal Processing**, v. 86, n. 1, p. 17-34, 2017.

BRUNO, L. Mechanical characterization of composite materials by optical techniques: A review. **Optics and Lasers in Engineering,** v. 104, p. 197-203, 2018.

DAL FABBRO, I. M. *et al.* Physical and mechanical properties of biological materials. **Engenharia Agrícola**, v. 51, n. 5, p. 1-9, 2020.

DOYLE, J. F. **Hybrid methods**. In: Springer Handbook of Solid Mechanics. Springer, 2008.

FUJITA, I. K.; ARAKI, S. Y. **Optics and VADs**. In: Bioengineering and Biomaterials in Ventricular Assist Devices. 1. ed. p. 325-333, 2021.

This article is published in open access under the Creative Commons Attribution 4.0 International (CC BY 4.0) license, which permits unrestricted use, distribution, and reproduction in any medium, provided that the original author and source are credited.

GAZZOLA, J. *et al.* Propriedades mecânicas dos materiais biológicos. **Ciências agrárias: o avanço da ciência no Brasil**, v. 2, n. 38, 2021.

GOMES *et al.* Calibração da técnica de *moiré* aplicada a perfilometria de protótipos mecânicos. **Ciência e Agrotecnologia**, v. 33, n. 2, p. 574-579, 2009.

HUBBLE, N.; WEAVER, L. Comparing shadow moiré and digital fringe projection warpage metrology techniques. **In: Proceedings of SMTA International 2017**. p. 1-11, 2017.

MAHIUDDIN, M. *et al.* Application of Caputo fractional rheological model to determine the viscoelastic and mechanical properties of fruit and vegetables. **Postharvest Biology and Technology**, v. 163, 111147, 2020.

MOHSENIN, N. N. **Physical properties of plant and animal materials: structure, physical characteristics, and mechanical properties**. 1. ed. Gordon and Breach Science Publishers, 1970.

NIGAM, R.; SINGH, S. K. Crack detection in a beam using wavelet transform and photographic measurements. **Structures**, v. 25, p. 436-447, 2020.

RASHVAND, M. *et al.* Numerical simulation as a tool for predicting mechanical damage in fresh fruit. Postharvest Biology and Technology, v. 187, 111875, 2022. DOI: 10.1016/j.postharvbio.2022.111875

SALARIKIA, A. *et al.* Finite element analysis of the dynamic behavior of pear under impact loading. **Information Processing in Agriculture**, v. 4, n. 1, p. 64-77, 2017.

SANCHEZ-ESPIGA, J. *et al.* Numerical evaluation of the accuracy in the load sharing calculation using strain gauges: Sun and ring gear tooth root. **Mechanism and Machine Theory**, v. 175, 104923, 2022.

SILVA, M. V. G. *et al.* Uso de técnicas ópticas de moiré para determinação prática do comportamento de vigas estruturais. **Revista Funec Científica**: Multidisciplinar, v.2, n. 3, 2012.

SILVA, M. V. G. *et al.* Application of optical method in measuring mechanical vibrations in a cantilever beam. **Engenharia Agrícola**, v. 37, n. 1, 2017.

SRIKLIN, W. *et al.* Stress-strain measurement of rubber with optical moiré fringes. **Journal of Physics**, v. 901, p. 012070, 2017.

STROPEK, Z.; GOLACKI, K. Viscoelastic response of apple flesh in a wide range of mechanical loading rates. **Int. Agrophys.**, v. 32, p. 335-340, 2018.

ZULKIFLI, N. *et al.* Finite element modelling for fruit stress analysis - A review. **Trends in Food Science & Technology**, v. 97, p. 29-37, 2020. DOI: 10.1016/j.tifs.2019.12.029.

This article is published in open access under the Creative Commons Attribution 4.0 International (CC BY 4.0) license, which permits unrestricted use, distribution, and reproduction in any medium, provided that the original author and source are credited.